

Novel Double Layer Salts of Copper(I) Bromide with N-Substituted Ethylenediammonium Cations

Roger D. Willett*

Department of Chemistry, Washington State University, Pullman, Washington 99164

Brendan Twamley

University Research Office, University of Idaho, Moscow, Idaho 83844

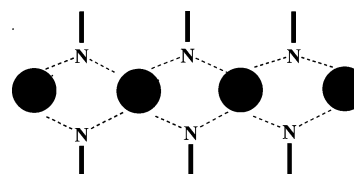
Received August 18, 2003

The structures of three hybrid organic/inorganic halometalate salts are reported, and the layer structures developed are contrasted. Crystal structures of the isostructural *N*-methylethylenediammonium (MEDA²⁺) and *N*-ethylethylenediammonium (EEDA²⁺) salts of copper(I) bromide are both triclinic, space group $P\bar{1}$, with lattice constants $a = 6.284(7)$, $b = 7.842(6)$, and $c = 12.03(1)$ Å, $\alpha = 84.84(3)$, $\beta = 83.08(2)$, and $\gamma = 88.00(3)^\circ$, and $V = 586(1)$ Å³ with $Z = 2$ for (MEDA)Cu₂Br₄ while (EEDA)Cu₂Br₄ has lattice constants $a = 6.27(2)$, $b = 7.78(2)$, and $c = 13.12(3)$ Å, $\alpha = 84.69(4)$, $\beta = 78.18(3)$, and $\gamma = 88.17(7)^\circ$, and $V = 623(3)$ Å³ with $Z = 2$. The dominant inorganic feature in both salts is anionic (CuBr₂)_{*n*}[−] chains of edge-shared CuBr₄ tetrahedra. The diammonium cations hydrogen bond these chains together into a unique double layer structure. For comparison purposes, the crystal structure of (CHA)PbBr₃ (CHA⁺ = cyclohexylammonium) is reported (monoclinic, space group $P2_1/n$, $a = 8.088(2)$ Å, $b = 7.912(2)$ Å, and $c = 19.572(4)$ Å, $\beta = 96.98(4)^\circ$, and $V = 1243.2(4)$ Å³ with $Z = 4$). This contains (PbBr₃)_{*n*}[−] halometalate chains, this time of face-shared PbBr₆ octahedra. However, here the organic cations tie the chains together into the more common single layer structure.

Introduction

The crystal chemistry of hybrid organic/inorganic halometalates is an important area of investigation, since such systems yield novel magnetic, conductive, thermo- and/or piezochromic, NLO, etc., materials. Much of the focus in this area has been on the intrinsic inorganic linkages that produce the desired physical effects. Many of these materials crystallize in well-defined low dimensional structures, e.g., layers or chains.¹ However, understanding the final crystalline structure of these materials depends as much, if not more, on the understanding of the secondary interactions, such as hydrogen bonding, π – π stacking, etc., present in the system. Thus, compounds with halometalate chains counterbalanced by non-hydrogen-bonding cations typically form hexagonal or pseudo-hexagonal structures in which each chain is surrounded by columns of six cations.² In contrast, com-

Chart 1



pounds that contain primary or secondary ammonium cations typically form layered structures in which the organic cations hydrogen bond the chains together into sheets, effectively forming bilayer structures, as illustrated diagrammatically in Chart 1.³ In this type of structure, the ionic components

* To whom correspondence should be addressed. E-mail: rdw@mail.wsu.edu.

(1) (a) Mitzi, D. B. *Prog. Inorg. Chem.* **1999**, *48*, 1. (b) Bloomquist, D. R.; Willett, R. D. *Coord. Chem. Rev.* **1982**, *47*, 125. (c) Willett, R. D. *NATO ASI Ser., Ser. C* **1985**, *No. 140*, 389.

(2) (a) Morosin, B.; Graeber, E. J. *Acta Crystallogr.* **1967**, *23*, 766. (b) Morosin, B. *Acta Crystallogr.* **1972**, *B28*, 2303. (c) Stucky, G. D. *Acta Crystallogr.* **1968**, *B24*, 330. (d) Clay, R. M.; Murray-Rust, P.; Murray-Rust, J. *J. Chem. Soc., Dalton Trans.* **1973**, 595. (e) Fujii, Y.; Wang, Z.; Willett, R. D.; Zhang, W.; Landee, C. P. *Inorg. Chem.* **1995**, *34*, 2870.

(3) (a) Groenendijk, H. A.; Blöte, H. W. J.; van Duyneveldt, A. J.; Gaura, R. M.; Landee, C. P.; Willett, R. D. *Phys. B+C (Amsterdam)* **1981**, *106B+C*, 47. (b) Caputo, R.; Willett, R. D. *Phys. Rev. B* **1976**, *13*, 3956. (c) Roberts, S. A.; Bloomquist, D. R.; Willett, R. D.; Dodgen, H. W. *J. Am. Chem. Soc.* **1981**, *103*, 2603.

are concentrated in the central portions of each layer and the organic portions form hydrophilic layers that sandwich the ionic portions.

One area of hybrid organic/inorganic chemistry that continues to provide a fertile area for structural research is that of the cuprous halide salts, due to the diverse coordination chemistry of the Cu(I) ion as well as the multiple bridging capabilities of the halide ions.⁴ A wide variety of oligomeric and polymeric species have been observed, based primarily on corner or edge sharing of planar CuX_3 or tetrahedral CuX_4 (regular or distorted) species.^{5–7} With a few exceptions, extended structures observed to date have been one-dimensional in nature,⁶ with only a couple of two-dimensional examples reported.⁷ The most common one-dimensional systems have contained single or double chains of edge-shared tetrahedral species, although many other, much more complex, structures have been observed. Most of the initial studies in this area have focused on counter-cations without hydrogen-bonding capabilities. It is clear that when hydrogen bonding is present, new constraints are placed on the system, and new and unusual structures can be obtained. Examples of this include the two layer structures recently obtained.⁷ It should be noted in passing that, in our laboratory, these species have most frequently been obtained serendipitously via autoreduction of Cu(II) halides in non-aqueous solvents or at elevated temperatures.^{7b,8}

In this article, we report on the structures of two such copper(I) bromide compounds obtained in our synthetic efforts in the preparation of copper(II) halide salts of N-substituted ethylenediammonium cations. The presence of

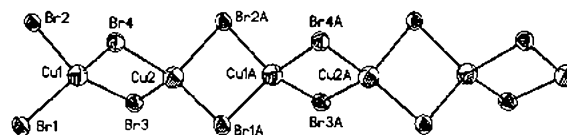


Figure 1. Illustration of the $(\text{CuBr}_2)_n^{2-}$ chain in $(\text{EEDA})\text{Cu}_2\text{Br}_4$. Thermal ellipsoids are shown at 50%. Selected bond distances (Å) and angles (deg) are as follows. $(\text{MEDA})\text{Cu}_2\text{Br}_4$: Cu1–Br1, 2.445(2); Cu1–Br3, 2.469(2); Cu1–Br4, 2.483(2); Cu1–Br2, 2.572(2); Cu2–Br3, 2.434(2); Cu2–Br2a, 2.500(2); Cu2–Br1a, 2.503(2); Cu2–Br, 2.524(2); Cu1–Br1–Cu2a, 80.18(9); Cu1–Br2–Cu2a, 77.86(9); Cu2–Br3–Cu1, 78.65(10); Cu2–Br4–Cu1, 76.73(10)°. $(\text{EEDA})\text{Cu}_2\text{Br}_4$: Cu1–Br1, 2.430(4); Cu1–Br3, 2.431(4); Cu1–Br4, 2.478(5); Cu1–Br2, 2.560(4); Cu2–Br3, 2.406(4); Cu2–Br2a, 2.485(4); Cu2–Br1a, 2.494(4); Cu2–Br4, 2.499(4); Cu1–Br1–Cu2a, 80.32(19); Cu1–Br2–Cu2a, 78.03(18); Cu2–Br3–Cu1, 79.77(19); Cu2–Br4–Cu1, 77.12(19).

two hydrogen-bonding moieties in the organic cation leads to a unique double layer structure. For comparison purposes, we report on a lead(II) halide structure that contains the more traditional single layer substructure.

Discussion

The structures of both $(\text{MEDA})\text{Cu}_2\text{Br}_4$ and $(\text{EEDA})\text{Cu}_2\text{Br}_4$ consist of tightly packed double layers of the diammonium cations and the $(\text{CuBr}_2)_n^{2-}$ chains. The cations in the MEDA and EEDA structures (not illustrated) assume all-trans conformations. The $(\text{CuBr}_2)_n^{2-}$ chains in both compounds consist of edge-shared tetrahedra, as illustrated in Figure 1 for the $(\text{CuBr}_2)_n^{2-}$ chain in EEDA structure. These tetrahedra show considerable variations, both in bond lengths and angles. The range of bond lengths is somewhat greater in the EEDA salt (2.406–2.560 Å) than in the MEDA structure (2.434–2.572 Å). The edge-shared structure causes the Cu–Br–Cu angles to be rather acute (76.7–80.3°) with Cu–Cu distances lying between 3.1 and 3.2 Å. These type of chains are not unique, with other systems containing $(\text{CuBr}_2)_n^{2-}$ chains having been reported in several instances.⁹ Nevertheless, there are subtle differences between the chains in the various compounds, probably attributable to the hydrogen-bonding capabilities (or lack thereof) of the counterions. Thus, in the paraquat salt, where no hydrogen bonding is present, the bridging Cu–Br–Cu angles are substantially smaller (67.9–72.5°), leading to shorter Cu–Cu distances than observed in these two structures.^{6g} In the substituted pyrazinium salt, an alternation of Cu–Br–Cu angles (and thus Cu–Cu) distances occurs.^{9b}

As illustrated in Figure 2 for $(\text{EEDA})\text{Cu}_2\text{Br}_4$, the double layers lie parallel to the *ab* planes in the crystal lattice. Each half of a double layer consists of alternating columns of the anionic chains and of the diammonium cations. In both structures, the diammonium cations are in all-trans conformations. The cations are oriented such that the $-\text{NH}_3^+$ headgroups penetrate into the layers and the $-\text{R}$ tails protrude out from the surface of the layers. In this manner, each diammonium cation hydrogen bonds to the bromide ions in three separate $(\text{CuBr}_2)_n^{2-}$ chains, utilizing a “bidentate bite” to hydrogen bond to two adjacent chains in half of the double

- (4) Subramanian, L.; Hoffmann, R. *Inorg. Chem.* **1992**, *31*, 1021.
 (5) (a) Asplund, M.; Jagner, S.; Nilsson, M. *Acta Chem. Scand. A* **1983**, *37*, 57. (b) Healy, P. C.; Engelhardt, L. M.; Patrick, V. A.; White, A. H. *J. Chem. Soc., Dalton Trans.* **1985**, 2541. (c) Pallenberg, A. J.; Koenig, K. S.; Barnhart, D. M. *Inorg. Chem.* **1995**, *34*, 2833. (d) Levy, A. T.; Olmstead, M. M.; Patten, T. E. *Inorg. Chem.* **2000**, *39*, 1628. (e) Andersson, S.; Jagner, S. *Acta Chem. Scand. A* **1987**, *41*, 230. (f) Asplund, M.; Jagner, S. *Acta Chem. Scand. A* **1984**, *38*, 135. (g) Andersson, S.; Jagner, S. *Acta Chem. Scand. A* **1985**, *39*, 423. (h) Andersson, S.; Jagner, S. *Acta Crystallogr., Sect. C* **1987**, *31*, 1089. (i) Asplund, M.; Jagner, S. *Acta Chem. Scand. A* **1985**, *39*, 47. (j) Hartl, H.; Brüdgam, I.; Mahdjour-Hassan-Abadi, F. *Z. Naturforsch.* **1985**, *40b*, 1032. (k) Hoyer, M.; Hartl, H. *Z. Anorg. Allg. Chem.* **1990**, *587*, 23. (l) Hu, G.; Holt, E. M. *Acta Crystallogr.* **1994**, *C50*, 1578. (m) Asplund, M.; Jagner, S. *Acta Chem. Scand. A* **1984**, *38*, 725. (n) Andersson, S.; Jagner, S. *Acta Chem. Scand. A* **1986**, *40*, 210. (o) Hartl, H.; Mahdjour-Hassan-Abadi, F. *Angew. Chem., Int. Ed. Engl.* **1984**, *23*, 378. (p) Andersson, S.; Jagner, S. *Acta Chem. Scand. A* **1989**, *43*, 39. (q) Hartl, H.; Mahdjour-Hassan-Abadi, F.; Fuchs, J. *Angew. Chem., Int. Ed. Engl.* **1984**, *23*, 514.
 (6) (a) Hu, G.; Holt, E. M. *Acta Crystallogr.* **1994**, *C50*, 1578. (b) Andersson, S.; Jagner, S. *Acta Chem. Scand. A* **1985**, *39*, 181. (c) Andersson, S.; Jagner, S. *Acta Chem. Scand. A* **1986**, *40*, 177. (d) Andersson, S.; Jagner, S.; Nilsson, M. *Acta Chem. Scand. A* **1985**, *39*, 447. (e) Asplund, M.; Jagner, S. *Acta Chem. Scand. A* **1984**, *38*, 129. (f) Batsanov, A. S.; Struchkov, Yu T.; Ukhin L. Yu; Dolgoplova, N. A. *Inorg. Chim. Acta* **1982**, *63*, 17. (g) Scott, B. L.; Willett, R. D.; Sacconi, A.; Sandrolini, F.; Ramakrishna, B. L. *Inorg. Chim. Acta* **1996**, *248*, 73. (h) Place, H.; Scott, B.; Willett, R. D. *Inorg. Chim. Acta* **2001**, *319*, 403.
 (7) (a) Place, H.; Scott, B.; Long, G.; Willett, R. D. *Inorg. Chim. Acta* **1998**, *279*, 1. (b) Willett, R. D. *Inorg. Chem.* **2001**, *40*, 966.
 (8) (a) Willett, R. D. *Inorg. Chem.* **1987**, *26*, 3423. (b) Place, H.; Willett, R. D. *Acta Cryst.* **1988**, *C43*, 34. (c) Willett, R. D. *Acta Crystallogr.* **1988**, *C43*, 450. (d) Willett, R. D.; West, D. X. *Acta Crystallogr.* **1987**, *C42*, 2300. (e) Willett, R. D.; Jettler, J. R.; Twamley, B. *Inorg. Chem.* **2001**, *40*, 6502. (f) Haddad, S.; Willett, R. D.; Twamley, B. *Acta Crystallogr.* **2000**, *C56*, e437.

- (9) (a) Sertuka, J.; Luque, A.; Lloret, F.; Roman, P. *Polyhedron* **1999**, *17*, 3875. (b) Scott, B.; Willett, R. D.; Porter, L.; Williams, J. *Inorg. Chem.* **1992**, *31*, 2483.

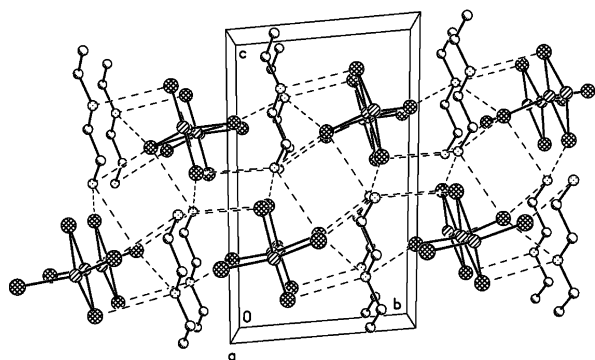


Figure 2. Illustration of the double layer structure in (EEDA) Cu_2Br_4 as viewed parallel to the a axis.

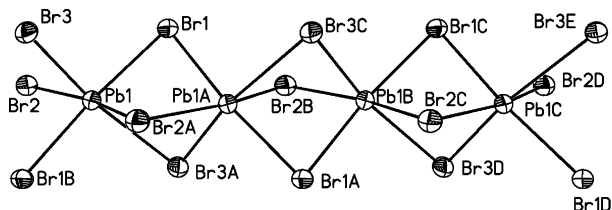


Figure 3. Illustration of the $(\text{PbBr}_3)_n^{n-}$ chain in $(\text{CHA})\text{PbBr}_3$. Thermal ellipsoids are shown at 50%. Selected bond distances (\AA): Pb1–Br1, 3.068(1); Pb1–Br1A, 3.005(1); Pb1–Br2, 3.148(1); Pb1–Br2A, 2.936(1); Pb1–Br3A, 3.313(1) \AA .

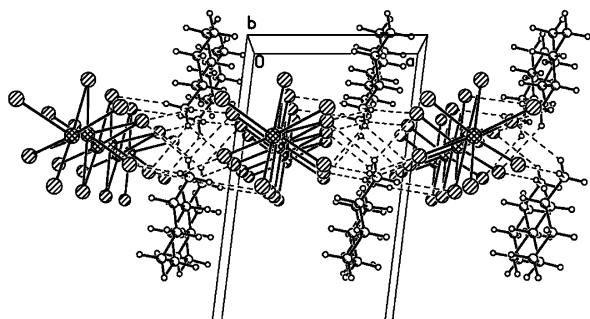


Figure 4. Illustration of the layer structure in $(\text{CHA})\text{PbBr}_3$ as viewed parallel to the b axis.

layer with the $-\text{NH}_3^+$ headgroup spanning across to a chain in the other half. In both compounds, the $-\text{NH}_3^+$ groups form two nearly linear $\text{N}-\text{H}\cdots\text{Br}$ hydrogen bonds and one asymmetric bifurcated hydrogen bond, while each $-\text{NH}_2^+$ group forms a single linear hydrogen bond and one asymmetric bifurcated hydrogen bond.

It is of interest to compare these two $(\text{REDA})\text{Cu}_2\text{Br}_4$ structures with the structures attained by monoammonium salts containing halometalate chains.³ For this purpose, we examine the structure of $(\text{CHA})\text{PbBr}_3$, where CPA^+ is the cyclohexylammonium cation. This contains a prototypical hybrid organoammonium halometalate chain structure observed when the cation is a primary or secondary ammonium ion. Figure 3 shows a portion of the $(\text{PbBr}_3)_n^{n-}$ chains of face-shared PbBr_6 octahedra that are found in this structure, while Figure 4 shows the hydrogen bonding with the cations that ties the chains together into layers. The cyclohexyl ring of the CPA^+ cation is in a boat conformation. The organic tails of the cations protrude well out from the ionic core of the layer, and these interdigitate to form the final crystal structure.

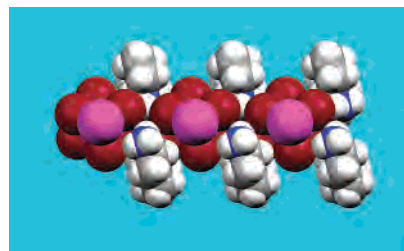


Figure 5. Space-filling illustration of the single layer structure in $(\text{CHA})\text{PbBr}_3$.

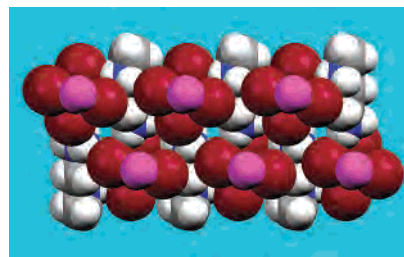
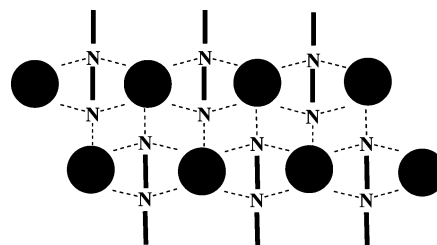


Figure 6. Space-filling illustration of the double layer structure in $(\text{MEDA})\text{Cu}_2\text{Br}_4$.

Chart 2



To compare the layer structures in the two systems, representations of the two types of layers are given in Charts 1 and 2 for the single and double layers respectively, while space-filling representations are shown in Figures 5 and 6 for $(\text{CHA})\text{PbBr}_3$ and $(\text{MEDA})\text{Cu}_2\text{Br}_4$, respectively. In the single layer structure, the $-\text{NH}_3^+$ group only penetrates partway into the halometalate layer. In contrast, the “bidentate” hydrogen-bonding bite of the diammonium cation allows the cation to penetrate through the halometalate layer so that the $-\text{NH}_3^+$ group is also able to hydrogen bond to a second layer, forming the double layer.

Experimental Section

The copper(I) compounds were obtained as colorless flat crystalline platelets in the crystallization of solutions containing a 1:2 $(\text{REDA})\text{Br}_2:\text{CuBr}_2$ ratio ($R = \text{Me}$ or Et) in ethanol/hydrobromic acid mixtures evaporated on a hot plate with temperatures held at 50–60 $^\circ\text{C}$. The solutions were partially covered during this process so that reduction of the volume occurred slowly. Similarly, the lead(II) salt was crystallized from a solution containing a 1.5:1 ratio of cyclohexylammonium bromide and lead(II) bromide dissolved in 1 M HBr .

X-ray Studies. Crystals were attached to a glass fiber using glue. Datasets were collected at 297(2) K using a Bruker/Siemens SMART 1K instrument (Mo $K\alpha$ radiation, $\lambda = 0.71073 \text{ \AA}$). Data were measured using ω scans of 0.3 $^\circ$

Table 1. Crystal Data and Structure Refinement Parameters

	C ₃ H ₁₂ Br ₄ Cu ₂ N ₂	C ₄ H ₁₄ Br ₄ Cu ₂ N ₂	C ₆ H ₁₄ Br ₃ PbN
empirical formula	C ₃ H ₁₂ Br ₄ Cu ₂ N ₂	C ₄ H ₁₄ Br ₄ Cu ₂ N ₂	C ₆ H ₁₄ Br ₃ PbN
fw	522.87	536.89	547.10
<i>T</i> (K)	303(2)	303(2)	301(2)
λ (Å)	0.710 73	0.710 73	0.710 73
cryst system	triclinic	triclinic	monoclinic
space group	<i>P</i> 1	<i>P</i> 1	<i>P</i> 2 ₁ / <i>n</i>
<i>a</i> (Å)	6.284(7)	6.268(15)	8.088(2)
<i>b</i> (Å)	7.842(7)	7.775(17)	7.912(2)
<i>c</i> (Å)	12.026(13)	13.12(3)	19.572(4)
α (deg)	84.84(3)	84.69(4)	90
β (deg)	83.08(2)	78.18(3)	96.98(4)
γ (deg)	88.00(3)	88.17(7)	90
<i>V</i> (Å ³)	585.8(10)	623(3)	1243.2(4)
<i>Z</i>	2	2	4
ρ_{calc} (Mg/m ³)	2.964	2.861	2.923
μ (mm ⁻¹)	17.222	16.193	23.164
indpdnt reflns	2004	2536	3431
R(int)	0.0059	0.0541	0.0584
<i>T</i> (max, min.)	0.7245, 0.1966	0.8548, 0.2468	0.249, 0.047
goodness-of-fit on <i>F</i> ²	0.910	0.910	0.980
R1	0.0420	0.0371	0.0408
wR2	0.0644	0.0762	0.0697

Table 2. Atomic Coordinates ($\times 10^4$) and Equivalent Isotropic Displacement Parameters ($\text{Å}^2 \times 10^3$) for (MEDA)Cu₂Br₄

atom	x	y	z	<i>U</i> (eq) ^a
Cu1	4997(2)	7674(1)	7310(1)	51(1)
Cu2	54(2)	7450(1)	7379(1)	48(1)
Br1	7452(1)	9931(1)	7545(1)	38(1)
Br2	7692(1)	5212(1)	6871(1)	36(1)
Br3	2275(1)	6783(1)	8893(1)	39(1)
Br4	2816(1)	8183(1)	5716(1)	36(1)
N1	1521(9)	12379(8)	5665(6)	39(2)
N2	3653(9)	12746(8)	8415(5)	36(2)
C1	2913(11)	13009(9)	6450(6)	33(2)
C2	2191(11)	12240(9)	7631(7)	34(2)
C3	3085(14)	11943(11)	9576(7)	50(2)

^a *U*(eq) is defined as one-third of the trace of the orthogonalized **U**_{*ij*} tensor.

frame for 30 s, and a half sphere of data was collected. The first 50 frames were recollected at the end of data collection to monitor for decay. Cell parameters were retrieved using SMART¹⁰ software and refined using SAINTPlus¹¹ on all observed reflections. Data reduction and correction for *Lp* and decay were performed using the SAINTPlus software. Absorption corrections were applied using SADABS.¹² The structures were solved by direct methods and refined by least-squares methods on *F*² using the SHELXTL program

(10) SMART: Bruker Molecular Analysis Research Tool, v.5.059; Bruker AXS: Madison, WI, 1997–98.

(11) SAINTPlus: Data Reduction and Correction Program; Bruker AXS: Madison, WI, 1999.

(12) Sheldrick, G. M. SADABS v.2.01: an empirical absorption correction program; Bruker AXS Inc.: Madison, WI, 1999.

Table 3. Atomic Coordinates ($\times 10^4$) and Equivalent Isotropic Displacement Parameters ($\text{Å}^2 \times 10^3$) for (EEDA)Cu₂Br₄

	x	y	z	<i>U</i> (eq) ^a
Cu1	4652(1)	7668(1)	7128(1)	49(1)
Cu2	−303(1)	7447(1)	7182(1)	47(1)
Br1	7086(1)	9944(1)	7304(1)	38(1)
Br2	7418(1)	5210(1)	6708(1)	35(1)
Br3	1667(1)	6813(1)	8568(1)	38(1)
Br4	2727(1)	8165(1)	5653(1)	35(1)
N1	1390(9)	12365(7)	5617(4)	38(1)
C1	2664(11)	13013(8)	6337(5)	34(2)
N2	3213(8)	12761(6)	8106(4)	28(1)
C2	1817(10)	12264(7)	7404(5)	30(1)
C3	2584(12)	11954(9)	9177(5)	43(2)
C4	4146(14)	12470(11)	9809(6)	65(2)

Table 4. Atomic Coordinates ($\times 10^4$) and Equivalent Isotropic Displacement Parameters ($\text{Å}^2 \times 10^3$) for (CPA)PbBr₃

atom	x	y	z	<i>U</i> (eq) ^a
Pb1	2530(1)	5112(1)	2420(1)	38(1)
Br1	4998(1)	2407(1)	2058(1)	43(1)
Br2	2641(1)	8051(1)	1343(1)	43(1)
Br3	5157(1)	7097(1)	3119(1)	44(1)
C2	7302(9)	2893(8)	3906(4)	41(2)
C3	7842(12)	1097(9)	3970(4)	59(2)
C4	7175(14)	244(10)	4567(5)	74(3)
C5	7603(13)	1178(12)	5223(4)	74(3)
C6	7023(16)	2962(12)	5145(5)	85(3)
C7	7747(13)	3846(10)	4562(4)	64(3)
N1	8053(8)	3746(7)	3339(3)	49(2)

package.¹³ No decomposition was observed during data collection. Structure refinements were straightforward in all three cases, and no disorder was observed. Data collection parameters are given in Table 1, and positional parameters are given in Tables 2–4. Further details are provided in the Supporting Information.

Acknowledgment. The assistance of Mr. Jason Jellison and Ms. Kathleen Reynolds in the syntheses is gratefully acknowledged. This work was supported in part by American Chemical Society PRF Grant 34779-AC5. The Bruker (Siemens) SMART CCD diffraction facility was established at the University of Idaho with the assistance of the NSF-EPSCoR program and the M. J. Murdock Charitable Trust, Vancouver, WA.

Supporting Information Available: Crystallographic data in CIF format. This material is available free of charge via the Internet at <http://pubs.acs.org>.

IC030260S

(13) Sheldrick, G. M. SHELXTL: Version 5.10, Structure Determination Software Suite; Bruker AXS Inc.: Madison, WI, 1998.